48th CIRP Conference on MANUFACTURING SYSTEMS - CIRP CMS 2015

Machining of thin-walled parts produced by additive manufacturing technologies

Isaev Alexander[a]*, Grechishnikov Vladimir[a], Pivkin Petr[a], Kozochkin Mihail[a], Ilyuhin Yuriy[a], Vorotnikov Andrey[a]

aMoscow State University of Technology "STANKIN", Vadkovskiy pereulok, 1, Moscow, 127005, Russia

* Corresponding author. Tel.: +7-916-180-6847; fax: +7-499-973-3071. *E-mail address:* a.isaev@stankin.ru

Abstract

The study aims at investigation of structure, properties and machinability rate of raw and thermal treated titanium-based powder material used to produce the thin-walled components by one of the most widespread additive manufacturing technologies, electron beam melting (EBM). The microstructure and material properties of raw EBM parts in horizontal cross-section and in vertical ones are different, i. e. the raw EBM samples structure and properties are anisotropic. To reduce anisotropy by modifying microstructure of EBM parts, a thermal treatment (hot isostatic pressing, HIP) was applied. In addition, when using additive manufacturing, the part surface roughness is quite coarse while the dimensions may be out of tolerance. Thus, making the end product after additive manufacturing often requires a finishing cutting operation. Examining the quality of end product in terms of geometric tolerance and thin walls thickness stability is also included in this study. In particular, when milling thin-walled parts produced by EBM technology, the form accuracy and the surface roughness are the functions of variable wall stiffness which is estimated in a local cutting zone. This fact must be taken into account when selecting the cutting conditions. For this purpose, a specially designed measuring information system has been used to control the vibrations during machining process.

1. Introduction

Nowadays, different types of additive manufacturing (AM) processes are extensively used to produce various kinds of machine components, including metal ones. One of the most widespread AM technologies is electron beam melting (EBM) which produces parts by melting metal powder layer by layer with an electron beam in a high vacuum. Unlike other techniques, e. g. direct metal laser sintering (DMLS), selective laser sintering (SLS) etc, parts made by the EBM are fully dense, void-free, and very strong.

Thin-walled parts are widely used in various products of aerospace, power engineering, fine mechanics and others, where light weight, high usability and ergonomics are required. In some cases, thin-walled components having complex geometry have to be produced using the AM technologies and further be machined either by "traditional" methods (turning, milling, grinding etc.), or by "non-traditional" ones, like electrical discharge machining or water jet cutting.

Milling is one of the most common machining method used in thin-walled part processing. Cutting and clamping forces acting during removal of chip produce the deflections of walls that are comparable with the machining stock thickness [1]. The specific microstructure of the parts made using the AM technologies causes additional instability of the machining process. Those deflections and process instability result in machining error that depends on wear of cutting tool, cutting conditions, parameters of the machine-workpiece-tool system, and other factors [2]. In practice, the type of milling (conventional or climb) dramatically influences the processing accuracy and machined surface roughness. Therefore, it is important to figure out how the machining errors vary with the change of operation conditions and material characteristics.

2. Material characterization

The raw (as-built) sample parts made of the VT-6 titanium alloy powder (equivalent to Ti6Al4V). with the average powder grain size ~70 μm using the Arcam A2 EBM system (Sweden) have the specific microstructure caused by the non-uniform thermal conditions of crystallizing and cooling of titanium alloy in vacuum chamber [3]. The X-ray diffraction phase analysis showed that the sample parts consist of the A2 type structure (β-Ti, up to 10% by volume) and the A3 type structure (α-Ti, up to 90% by volume). The typical microstructures of the raw parts in different cross-sections are shown in Fig. 1. This microstructures are characterized with specific stroke pattern. When melting the powdered metal, the grains of β-Ti stretch along the direction of the metal flow. During cooling the parts in the vacuum chamber, when the temperature goes down to the α-Ti precipitation, the rate of β-Ti growth slows down. Regardless the cooling rate, the α-Ti phase precipitates on the β-Ti defects and along the metal flow. In Fig. 1 (a) the microstructure of the layer parallel to the horizontal XY plane (base plane) where the melting is performed, is shown. In Fig. 1 (b), long white horizontal lines correspond the part's layers, while vertical lines coincide with the tracks columns.
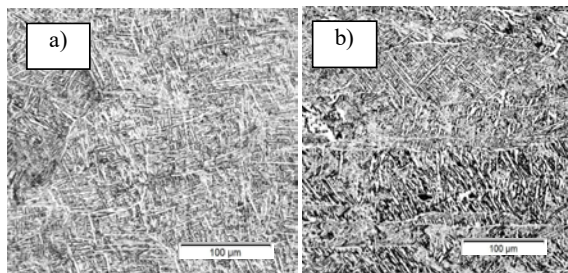

Fig. 1. Microstructure of parts produced by the Arcam A2 EBM system in cross-section planes: a) XY; b) YZ.

The raw material characterization in different cross-section planes is shown in Table 1. As it is shown there, the content of α-Ti and β-Ti depends on the cross-section plane orientation.

Table 1. VT-6 titanium alloy characterization

Phase	Lattice parameter, Å	Volume ratio in XY plane	Weight content in XY plane	Volume ratio in ZY plane	Weight content in ZY plane	Volume ratio in ZX plane	Weight content in ZX plane
β-Ti	a=2.92, c=4.683	7.0±0.2	7.3±0.2	4.9 ± 0.1	5.1±0.1	10.0±0.1	10.4±0.1
α-Ti	a=2.912	93.0±0.2	92.7±0.2	95.1±0.1	94.9±0.1	90.0±0.1	89.6±0.1

At the same time, regardless the cross-section plane orientation, the same structure can be seen in the microsection. On the former β-Ti grain boundaries the spherical α-Ti grains start to grow, as shown in Fig. 2 (a). With the cooling rate increasing (possibly when the electron beam moves away from the melting region), the new α-Ti grains becomes platy (Widmanstätten patterns). Between the plates of α-Ti some

retained β-Ti grains can be observed, whilst the α-Ti grains contains a few number of micro-inclusions, that could be either needle-like precipitates of α-Ti oriented normally to the surface of microsection, or some unknown third phase.

The precipitating α-phase has the larger grain size. This is the reason of residual tensile stresses in the end product. Thus, the recrystallization annealing to lower these stresses is recommended. In the present work, the hot isostatic pressing (HIP) was applied to the sample part (hot isostatic press AIP8-30H (USA), 920 °C, 1000 Bar, 120min). The microstructure after the HIP is shown in the Fig. 2 (b). It is obvious that the structure became much more homogenous in all cross-section planes. Consequently, the mechanical properties of the part are more isotropic than in the raw material. On the other side, the effect of HIP is just about 3—4%. Actually, this small difference in properties between HIP and raw is an indication of a defect-free product.
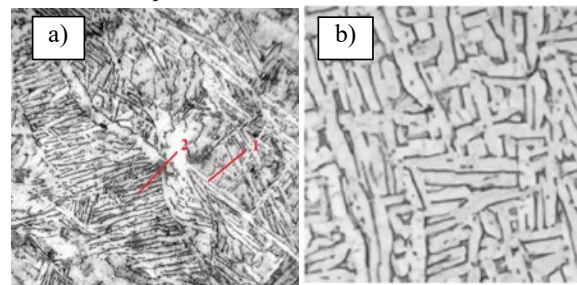

Fig. 2. (a) Raw material (200x); (b) heat treated material (500x).

3. Experimental procedure

The geometric parameters of the EBM-parts don't match the initial 3D model. In addition, the side faces of the EBM-parts have stochastic irregular surface. Thus, to provide the end product quality, it is necessary to machine the parts using some 'traditional' methods like milling or grinding [4].

A sample part to be machined during the experiment is shown in Fig. 3 (a). Total part's height is 18 mm. Four series of experiments were conducted with the wall thickness t of 1.5 mm, 1.0 mm, 0.5 mm and 0.3 mm. Finishing cutting speed: 188 m/min; feed rate: 0.03 mm/tooth; depth of cut: 0.5 mm; width of cut: 3.6 mm. The part was machined downwards in 5 passes. Walls thickness measurement scheme is shown in Fig. 3b. To measure vibrations generated during the machining process, a measuring information system has been used [5].
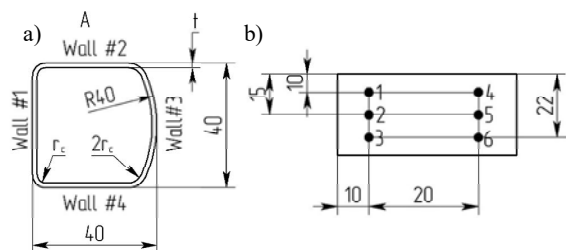

Fig. 3. (a) Sample part; (b) walls thickness measurement scheme.

The line graph in Fig. 4 (a) shows that relatively thick walls (t=1.5 mm) gets thicker towards the bottom of the workpiece, especially for conventional milling, because in this type of milling a normal component of cutting force acts towards the axis of the cutter making the cutter's body to slightly increase its radial runout and to deviate from the relatively stiff wall being machined. While the point of contact between the cutting edge and the part's surface moves downwards during the machining process, the wall's stiffness increases and the cutter's deviations and runout become smaller, that leads to increasing wall's thickness towards the bottom. In addition, the chips disposed before the cutter can also affect the milling cutter and increasing the thickness of the walls. In climb milling, the width of the cut starts at the maximum producing less friction forces [6]. The normal component of the cutting force acts in a direction of the relatively stiff wall. The chips are disposed behind the cutter. This provides less cutter's deviations and hence less walls thickness variation.

This situation changes as the walls are getting thinner and their stiffness decreases, as shown in Fig. 4 (b). In this case, the walls deform more than the cutter does. In climb milling, the top part of the walls deviates from the cutter's body and gets thicker than their lower part. Conversely, in conventional milling the walls become thicker to the bottom part of the workpiece, and the wall's mean thickness is closer to its nominal value.
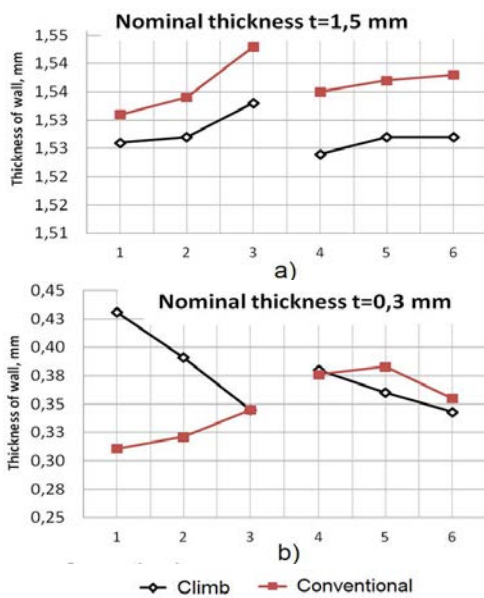

Fig. 4. Walls thickness variations depending on the measuring point and milling type.: (a) for nominal wall's thickness of 1.5 mm; (b) for nominal wall's thickness of 0.3 mm.

The roughnesses of the wall #1 and the smaller inner corner surface was performed using the contact profilometer. The climb milling provides slightly better roughness (Ra=0.2—0.4 μm) than the conventional one (Ra=0.3—0.7 μm) when machining relatively thin walls (0.5 mm or thinner). Both conventional and climb milling produces very rough surface in the corners of small radii in comparison with the rest of surfaces being machined (Ra=2.0—7.8 μm). Though the roughness of the curved surface of relatively big radius (the wall #3) couldn't be measured directly with a contact profilometer, it has obviously a better roughness than other surfaces of the sample part. It can be explained by the higher stiffness on the curved wall that produces less chattering of the elastic system "machine-tool-workpiece".

Surfaces of the walls with t=0.3 mm machined under different cutting conditions are shown in Figure 5. In Fig. 5 (a), the periodic milling marks left after climb milling are visible. In Fig. 5 (b), the wall machined by conventional milling where there is a lot of spots left by chip, is shown. Fig. 5 (c) represents the curved wall #3 which has visibly lower roughness than other surfaces. Fig. 5 (d) shows a very rough surface in the corner of small radius which is equal to the radius of the milling cutter.
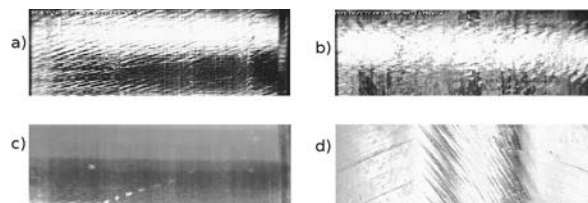

Fig. 5. Surfaces of the walls with t=0.3 mm: (a) climb milling; (b) conventional milling; (c) climb milling of the curved wall; (d) climb milling of the corner with a small radius.

4. Vibroacoustic signal analysis

During the milling process a vibroacoustic signal was recorded using the accelerometer installed on the machine's table [7]. The samples of the vibroacoustic signal for conventional and climb milling are shown in Fig. 6. In conventional milling, non-repetitive accidental peaks of up to 0.3 ms width have been observed. These peaks are caused by chip disposed before the milling cutter, as it was shown above, and result in a poor appearance of the wall's surface (spots and strokes), although a roughness parameter Ra has not been significantly changed on these parts of surface. The appearance of the waveform both for raw and heat treated materials is highly similar.
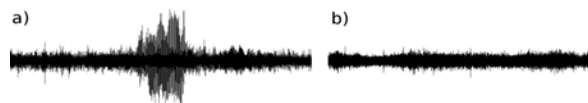

Fig. 6. Vibroacoustic signal for: (a) conventional milling; (b) climb milling.

The vibration acceleration spectra for climb and conventional milling are represented in Figure 7a and 7b, respectively. These waveforms were obtained for the last pass of the cutter that has been moved along the bottom surface of the workpiece, where a large amount of chip affects the machining process.

The spectra presented in Fig. 7 have their maximum amplitudes at double tooth frequency ($2f_{tooth}$) and the local

maximum amplitudes at frequencies multiple to the cutter's rotation one (f_{rot}). However, for the conventional milling the amplitude of vibroacoustic signal at high frequencies is significantly lower than the maximum at $2f_{tooth}$. It means decrease of impacts when the teeth enter and exit the workpiece which is caused by the chip-disposal effect described above.
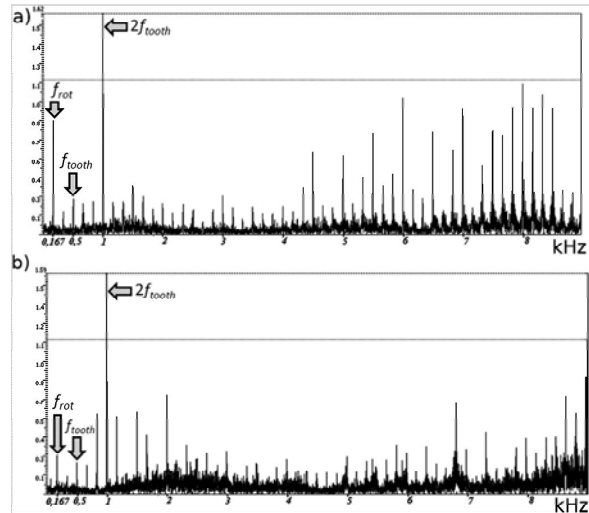

Fig. 7. Vibration acceleration spectra: (a) climb milling; (b) conventional milling.

5. Summary

As the study results show, the microstructure and material properties of EBM parts in the base horisontal plane and in vertical ones are different, i. e. the raw EBM samples structure and properties are anisotropic. Annealing of the parts produced by EBM have no significant affect to machining process and the resulted surface properties;

When milling EBM thin-walled parts, the form accuracy and the surface roughness are the functions of variable wall stiffness which is estimated in a local cutting zone. This fact must be taken into account when selecting the cutting conditions.

The milling of surfaces with a low stiffness is a dynamically unstable process which produces vibrations (chattering) and relatively big displacements of the cutter and the workpiece. When using conventional milling these vibrations are lower, but the surface roughness is significantly higher because of the chip disposed to the cutting zone.

When designing thin-walled parts, it is desirable to replace flat surfaces with the curved ones, if possible, as the curved surface provides a higher stiffness and hence a better surface roughness and a less form deviations;

Use of vibroacoustic analysis when development of technological process of thin-walled parts machining seems to be feasible as it helps to efficiently detect and estimate the undesirable effects.

Acknowledgements

References

[1] Grechishnikov V A, Isaev A V and Markos S 2007 Designing assembled milling cutters for machining the profiled surfaces. Rus. Eng. Res. 27 291–293
[2] Grechishnikov V A and Isaev A V 2010 Machining curvilinear sections by means of cutting plates with a linear edge. Rus. Eng. Res. 30 413–417
[3] Luis A Díaz, Miguel A Montes-Morán, Pavel Y Peretyagin, Yuriy G Vladimirov, Anna Okunkova, José S Moya and Ramón Torrecillas 2014 Zirconia–alumina–nanodiamond composites with gemological properties. J. of Nanopart. Res. 16 DOI 10.1007/s11051-014-2257-x
[4] Shaw M C 2005 Metal Cutting Principles (New York: Oxford University P.)
[5] Kozochkin M P, Kochinev N A and Sabirov F S 2006 Diagnostics and monitoring of complex production processes using measurement of vibration-acoustic signals. Meas. Techniques, 49 672–678
[6] Volosova M A and Gurin V D 2013 Influence of vacuum-plasma nitride coatings on contact processes and a mechanism of wear of working surfaces of high-speed steel cutting tool at interrupted cutting J. of Frict. and Wear. 34 183–189
[7] Isaev A V and Kozochkin M P 2014 Use of a measurement information system to increase the precision with which thin-walled parts are machined on numerically controlled milling machines. Meas. Techniques, 56 1155–61.